THE ASTROPHYSICAL JOURNAL, 412:278–287, 1993 July 20

CP PUPPIS: NO ORDINARY OLD NOVA

JAMES C. WHITE II[1] AND R. KENT HONEYCUTT[2]
Department of Astronomy, Indiana University, Bloomington, IN 47405

AND

KEITH HORNE
Space Telescope Science Institute,[3] 3700 San Martin Drive, Baltimore, MD 21218
Received 1992 November 3; accepted 1993 January 22

ABSTRACT

We present spectrophotometric data for the old nova CP Puppis (Nova Puppis 1942) that demonstrates the simultaneous existence of two distinct periods for the system. We find that the photometric period of 0.06834(7) day is 11% longer than the spectroscopic period. We also present Doppler tomographic images of CP Pup that indicate the existence of an accretion disk in the system. Finally, we interpret the observational evidence in terms of a DQ Herculis model and an SU Ursae Majoris model for CP Pup. While the evidence mildly supports both interpretations, it is insufficient for us to conclusively classify CP Pup as either a DQ Her system or an SU UMa system.

Subject headings: accretion, accretion disks — binaries: close — novae, cataclysmic variables — stars: individual (CP Puppis)

1. INTRODUCTION

In spite of all the observations devoted to CP Puppis (Nova Puppis 1942), it still remains a mysterious object. The very fast, yet smooth, decline from outburst of 3 mag in 6.5 days (Payne-Gaposchkin 1957) identified CP Pup as an unusually fast nova; further, its brightness increase of approximately 17 mag during outburst placed it within the range of supernovae, yet as Weaver (1944) noted, its spectrum bore no resemblance to those of supernovae. Since then we have come to view CP Pup as a member of the large class of interacting binary stellar systems collectively referred to as cataclysmic variables (CVs). The generally accepted model of a generic CV consists of a late-type dwarf star transferring material to its white dwarf companion via Roche-lobe overfill. In systems where the white dwarf is not magnetized, the material from the secondary star forms an accretion disk around the degenerate primary star (Robinson 1976a; Bath & Pringle 1985; Wade & Ward 1985); however, in systems where the white dwarf is magnetized, the accretion disk is disrupted near the white dwarf surface or prevented from forming at all (Warner 1983; Liebert & Stockman 1985; Wickramasinghe 1988).

Magnetized CVs are divided into two classes based on the magnetic field strength of the white dwarf and synchronization (or lack thereof) of the orbital period with the white dwarf's spin period. DQ Herculis systems, or "intermediate polars," are characterized by magnetic field strengths $\lesssim 10$ MG and nonsynchronization of the white dwarf spin period and system orbital period (Berriman 1988), while AM Herculis systems, or "polars," are synchronous systems (Schmidt & Stockman 1991) with field strengths of tens of MG (Schmidt & Liebert 1987). Accretion funnels, rather than accretion disks, are found in AM Her systems; the strong magnetic field forces the infalling gas from the secondary star onto one or two magnetic poles on the white dwarf. In DQ Her systems, the weaker magnetic field disrupts the accretion disk near the white dwarf's surface, and the material within the inner disk radius is constrained to accretion funnels.

Recent photometric and spectroscopic studies of CP Pup at visible wavelengths (Bianchini, Friedjung, & Sabbadin 1985; Warner 1985a; Duerbeck, Seitter, & Duemmler 1987; Friedjung, Bianchini, & Sabbadin 1988; Barrera & Vogt 1989; O'Donoghue et al. 1989; Diaz & Steiner 1991) and infrared wavelengths (Szkody & Feinswog 1988) have identified characteristics of this nova that appear to place it in the DQ Her class. Warner (1985a) determined a photometric period of 0.06196 day or its 1 day alias 0.06614 day, while Vogt et al. (1990) determined a photometric period range of 0.059 day to 0.070 day over several nights of observations. O'Donoghue et al. (1989, hereafter OWWG) determined a period of 0.06143 day from their photometric observations, but while their period differs from Warner's (1985a) by 0.00053 day, it differs from Warner's 1 day alias by 0.0047 day, substantially greater than the uncertainty on either determination. This suggests the existence of more than one photometric period or the masking of the true white dwarf spin period by a beat period (Vogt et al. 1990). This multiplicity in CP Pup's photometric periods, a characteristic of other nonsynchronized magnetic CVs (Warner 1985b), combined with a lack of measurable circular polarization (Cropper 1986; Stockman, Schmidt, & Lamb 1988), much less modulation in circularly polarized light, suggests that CP Pup may be a DQ Her system.

In this paper we present spectrophotometric data on CP Pup collected in 1987 January at CTIO. We find simultaneous, yet distinctly different, spectroscopic and photometric periods for the system. Although Duerbeck et al. (1987) stated that there was little doubt that CP Pup's spectroscopic period is shorter than its photometric period, the work of OWWG suggested that the spectroscopic and photometric periods were equal to within the errors. We find at our epoch at least that the spectroscopic period is shorter than the photometric period by $\sim 11\%$. Such a disparity between periods has been observed in the old nova V603 Aquilae (Haefner 1981), and

[1] e-mail: whitejac@indiana.EDU.
[2] Visiting Astronomer, Cerro Tololo Inter-American Observatory, which is operated by the Association of Universities for Research in Astronomy, Inc., under cooperative agreement with the National Science Foundation.
[3] Operated by the Association of Universities for Research in Astronomy, Inc., under contract with the National Aeronautics and Space Administration.

more recently in the nova-like variable V795 Herculis (PG 1711+336; Shafter et al. 1990). We observe like Warner (1985a) a periodic variation in CP Pup's light curve with an amplitude of approximately 0.3 mag peak-to-peak; such behavior, coupled with the observed "standstill" in system brightness (Bianchini 1990) following outburst and an orbital period that places it below the period gap for CVs, is strongly reminiscent of superhumps in SU Ursae Majoris systems during a protracted superoutburst (Warner 1985c). Thus, the evidence we present suggests that CP Pup may be a member of either the DQ Her class or the SU UMa class of CVs.

2. OBSERVATIONS

Time-sequenced spectrophotometry of CP Pup was obtained on the nights of 1987 January 17 and 18 (UT), using the Cassegrain Spectrograph and the Two-Dimensional Photon Counter on the 4 m telescope at CTIO. With a slit width of 1".7 and transparency and seeing of high quality and stability both nights, we were able to extract good light curves from our data. The wavelength range was 3500–5000 Å, and the full width at half-maximum (FWHM) resolution was 2.5 Å. Exposure times were 300 s, and the typical spacing of the exposures was 340 s with occasional longer interruptions for calibrations. On each night approximately 55 CP Pup spectra were obtained over ~5.5 hr. Spectrophotometric standard stars were observed several times each night, and wavelength calibration spectra were obtained at the beginning, middle, and end of each 5.5 hr sequence.

Spectral reductions consisted of flat-field calibration, extraction of one-dimensional spectra from the two-dimensional images, wavelength calibration, sky subtraction, and flux calibration. The reductions were performed using the Image Reduction and Analysis Facility (IRAF) and were relatively straightforward with two exceptions. First, wavelengths bluer than ≈3750 Å suffered from an inconsistent flux calibration as well as an uncertain wavelength scale due to a scarcity of UV lines in the calibration lamp. Therefore, only the region ≈3750–5000 Å was retained for analysis. Second, the wavelength zero-point underwent a discontinuous change of ≈3 pixels (≈3 Å) on each of the two nights. On both occasions the change occured sometime between the middle and ending wavelength calibration spectra for each 5.5 hr sequence. Fortunately, it was possible to disentangle this wavelength change from possible changes in CP Pup itself by using the sky spectra which were extracted as a by-product of the reductions. The moon was bright during the observations; this enabled us to use the H and K absorption lines in the sky spectra to pinpoint the time and amplitude of the discontinuity. The change occurred at an hour angle of 2:45 W each night, implying that it was probably due to a mechanical shift of some sort as the telescope tracked westward. With the application of this correction to the data, the radial velocities for CP Pup appear well behaved and without discontinuities. Nevertheless, the necessity of this correction diminishes our trust in our derived γ-velocities for CP Pup.

3. ANALYSIS

3.1. *Photometry*

The photometry of CP Pup was obtained by excluding the emission lines and integrating the continuum flux for each of the 105 spectra over the *B*-band wavelength range 4400 ± 490 Å. Using our spectroscopic ephemeris of § 3.2 ($P = 0.06129$),

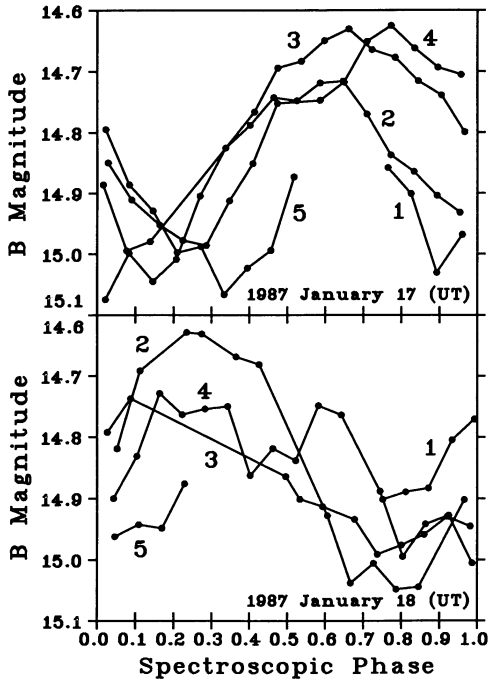

FIG. 1.—*B*-band light curve of CP Pup as a function of spectroscopic phase for 1987 January 17 and 18. Solid lines connect continuous data, and the time order of each set is indicated.

we show CP Pup's light curve as a function of spectroscopic phase in Figure 1. The photometric maxima for the two nights of data occur at different spectroscopic phases, indicating the existence of a photometric period distinctly different from the spectroscopic period. Furthermore, there is a systematic shift of the light curve from orbit to orbit within a night. The power spectrum for our photometric data (Fig. 2*a*) clearly shows a peak at 0.068 day with 1 day aliases of 0.074 day and 0.064 day. The rms fits of sinusoids to the data for the 1 day aliases 0.074 day and 0.064 day, 0.078 mag and 0.065 mag, respectively, are significantly larger than that of 0.055 mag for the 0.068 day period. We also derived photometric periods for the two nights separately: for the first night we find $P = 0.0675(3)$ day and for the second night $P = 0.0672(8)$ day. The difference between the periods for the two nights separately and that for both nights combined is not significant to within the errors. In light of these results, we adopted a photometric period of 0.06834(7) day that is substantially different from that of OWWG and somewhat different from that of Warner (1985a). Figure 3 shows the best-fit sinusoid and the data using our photometric ephemeris

$$\mathrm{HJD} = 2{,}446{,}812.0254 + 0.06834E\,, \quad \pm 1 \qquad \pm 7$$

where photometric phase $\phi_p = 0$ corresponds to the midpoint between minimum and maximum of the sinusoid fit.

3.2. *Radial Velocity Study*

We measured radial velocities for CP Pup using a least-squares routine that fitted selected lines with Gaussians. To avoid problems of possible contamination of line cores from

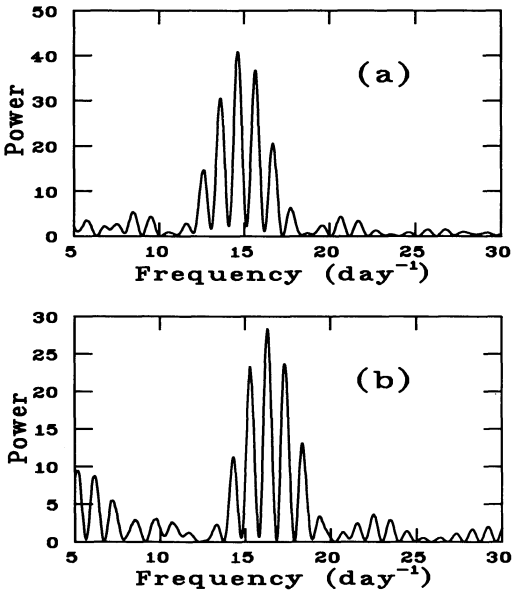

FIG. 2.—(*a*) Power spectrum of the photometry in Fig. 1. The mean brightness of each night's data was removed before Fourier analysis. The dominant peak in the spectrum at 14.6 day^{-1} corresponds to a photometric period of 0.068 day. (*b*) Power spectrum from the radial velocity analysis of § 3.2. The dominant peak in the spectrum at 16.3 day^{-1} corresponds to a spectroscopic period of 0.061 day.

asymmetric emission sources in the system (OWWG), we fitted each line several times, each fit performed with a different line-core width c(Å) excluded. Shown in Figure 4 for Hβ are K_1 and σ_{K_1}/K_1 as functions of the excluded region c, where K_1 is the white dwarf radial velocity and σ_{K_1} is the error on K_1. In a manner similar to that of other authors (Schneider & Young 1980; Shafter & Szkody 1984; Kaitchuck et al. 1987) we take as the best estimate of K_1 the value at the point at which σ_{K_1}/K_1 begins to increase dramatically. Therefore, for the data of Figure 4, we would choose a best K_1 velocity of 94 $\pm$ 6 km s^{-1}.

Initially, we made radial velocity curve fits separately for the two nights. The night-to-night differences in the velocity curve parameters for a given line were often larger than the errors for the parameters from a given night, indicating that the emission lines probably changed between the two nights. However,

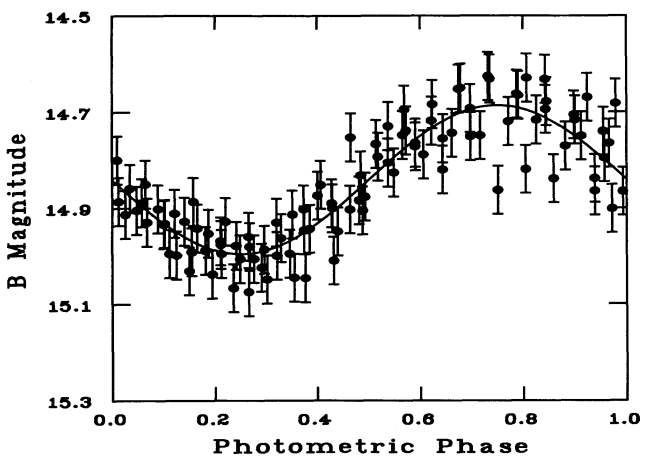

FIG. 3.—Light curve data of Fig. 1 and its best-fit sinusoid folded on the photometric ephemeris of § 3.1 for which $\phi_p = 0$ corresponds to the midpoint between minimum and maximum of the sinusoid fit.

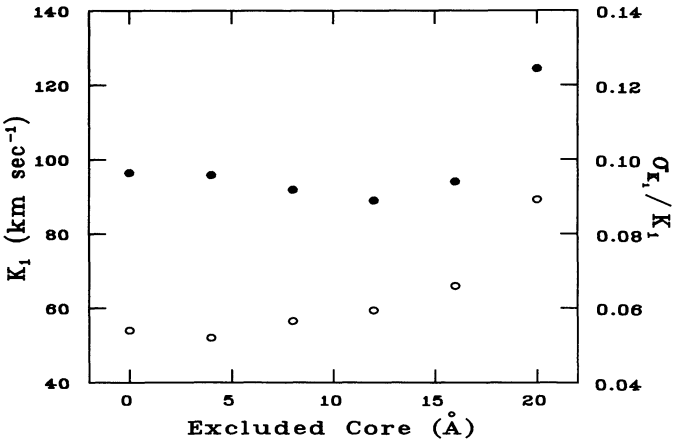

FIG. 4.—K_1 (*filled ovals*) and σ_{K_1}/K_1 (*open ovals*) for Hβ as a function of the excluded line core width.

there were no systematic differences (to within the errors) in K_1, γ, and ϕ_0 between the two nights when we considered collectively all the emission lines in Table 1. Therefore, Table 1 lists the best-fit parameters for the combined data of the two nights obtained using the equation

$$v(\phi_s) = \gamma - K_1 \sin [2\pi(\phi_s - \phi_0)] , \quad (1)$$

where ϕ_s is spectroscopic phase.

In Table 2 we list published values of K_1 for CP Pup. Our results for some individual lines compare quite well to those of OWWG, but not as well to those of Duerbeck et al. (1987) who determined a K_1 of 92 $\pm$ 18 km s^{-1} using Hα, Hβ, and He II λ4686, and Barrera & Vogt (1989) who found a K_1 of 85 $\pm$ 6 km s^{-1} using the H Balmer series and He II λ4686. These latter two results, however, are equivalent to our K_1 for Hβ and He II λ4686 (Table 1) within the errors. We combined the six velocities of the H Balmer lines (Hβ, Hγ, Hδ, Hϵ, H8, and H9) and performed a fit in the manner previously described. The result for the combined lines, 146 $\pm$ 6 km s^{-1}, is included in Table 2 and shown graphically in the top panel of Figure 5. Although our estimate of K_1 for the H Balmer lines is the same as that for the He I lines to within the errors, the variablity in our K_1 estimates among the lines is striking. OWWG also noted such variations in K_1 among the H Balmer, He I, and He II lines. The range in our estimates from 85 $\pm$ 4 km s^{-1} for He II λ4686 to 177 $\pm$ 14 km s^{-1} for H9 indicates that systematic differences from line to line dominate the statistical

TABLE 1

RADIAL VELOCITIES IN CP PUPPIS

Spectral Lines	γ (km s^{-1})	ϕ_0	K_1 (km s^{-1})	c (Å)
H Balmer Series:				
Hβ	-3 ± 4	0.01 ± 0.01	94 ± 6	16
Hγ	-3 ± 6	0.04 ± 0.01	127 ± 8	16
Hδ	-6 ± 6	0.01 ± 0.01	142 ± 8	12
Hϵ	-5 ± 6	0.03 ± 0.01	174 ± 8	12
H8	-1 ± 6	0.04 ± 0.01	161 ± 9	8
H9	-2 ± 10	0.03 ± 0.01	177 ± 14	8
He I:				
λ4471	-6 ± 14	-0.01 ± 0.02	171 ± 20	4
λ4026	38 ± 18	0.01 ± 0.02	157 ± 25	8
He II:				
λ4686	-3 ± 3	0.02 ± 0.01	85 ± 4	8
λ4541	-4 ± 13	0.06 ± 0.02	136 ± 18	8

TABLE 2

K_1 AND COMPONENT MASSES FOR CP PUPPIS

Reference	K_1 (km s^{-1})	M_1 ($M_\odot$)	M_2 ($M_\odot$)	$f(M_2)$ ($M_\odot$)
Duerbeck et al. 1987[a]	92 ± 18	0.12	0.14	0.0049 ± 0.0028
O'Donoghue et al. 1989[b]	$\gtrsim 120$	<0.4	0.11	...
Barrera & Vogt 1989[c,d]	85 ± 6	0.6	0.15	...
Vogt et al. 1990[c,d]	85 ± 6	0.6	0.15	...
This study[e]	146 ± 6	<0.18	0.14	0.020 ± 0.0024
Bianchini et al. 1990[a,f]	70	...	...	...

[a] K_1 determined using Hα, Hβ, and He II λ4686.
[b] K_1 determined using Hβ, Hγ, Hδ, Hϵ, H8; M_1 estimated from authors' Fig. 6.
[c] K_1 determined using Balmer series and He II λ4686.
[d] 1989 and 1990 papers treat the same data.
[e] K_1 determined using Hβ, Hγ, Hδ, Hϵ, H8, H9.
[f] Estimated from authors' Fig. 1.

uncertainties in the radial velocity fits. Hence, we believe our estimates of K_1 are not an accurate indicator of white dwarf orbital motion. We nevertheless adopt the half-amplitude for the combined H Balmer emission lines as K_1. To prevent any cycle count ambiguity between our epoch and those of the published spectroscopic ephemerides, we derived from our data alone the linear spectroscopic ephemeris

$$T_0 = 2{,}446{,}812.5961 + 0.06129E\,,$$
$$\pm 1 \qquad \pm 1$$

where T_0 is the plus to minus γ-crossing of the H Balmer emission-line radial velocity curve (see Fig. 5), and the spectroscopic period 0.06129 day corresponds to the maximum power peak at 16.3 day^{-1} in the power spectrum shown in Figure 2*b*.

Finally, to search for any contribution to our determinations of K_1 from dynamical sources other than orbital motion of the white dwarf, we folded the radial velocities of the H Balmer lines on our photometric ephemeris. The results of this exercise are shown in the top panel of Figure 6, along with the best-fit sinusoid of semiamplitude 41 ± 11 km s^{-1}. We note that while

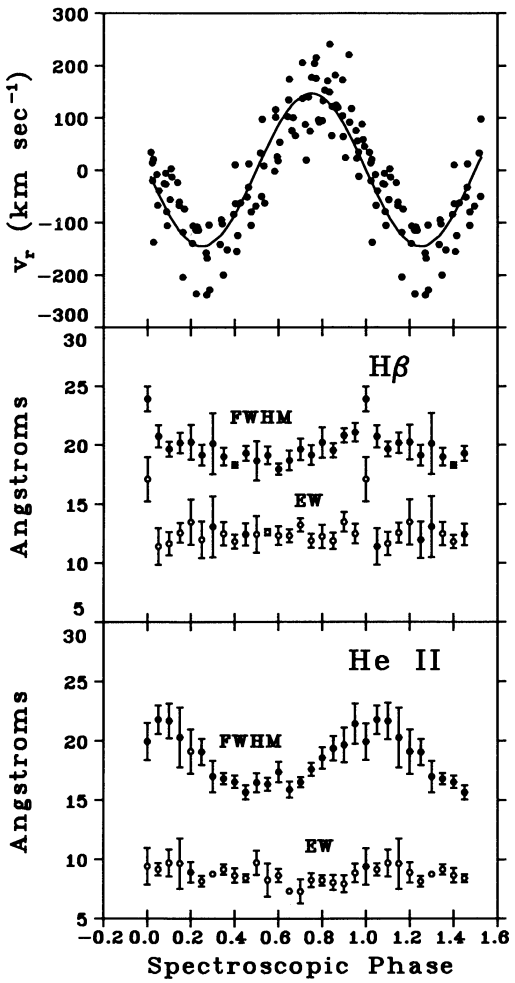

FIG. 5.—*Top panel:* Radial velocity curve for six H Balmer lines plotted as a function of spectroscopic phase. The solid line is the best-fit sinusoid with a semiamplitude of 146 km s^{-1}. *Middle panel:* FWHM (*filled ovals*) and equivalent width (EW; *open ovals*) for Hβ as a function of spectroscopic phase. *Bottom panel:* FWHM (*filled ovals*) and equivalent width (*open ovals*) for He II λ4686 as a function of spectroscopic phase.

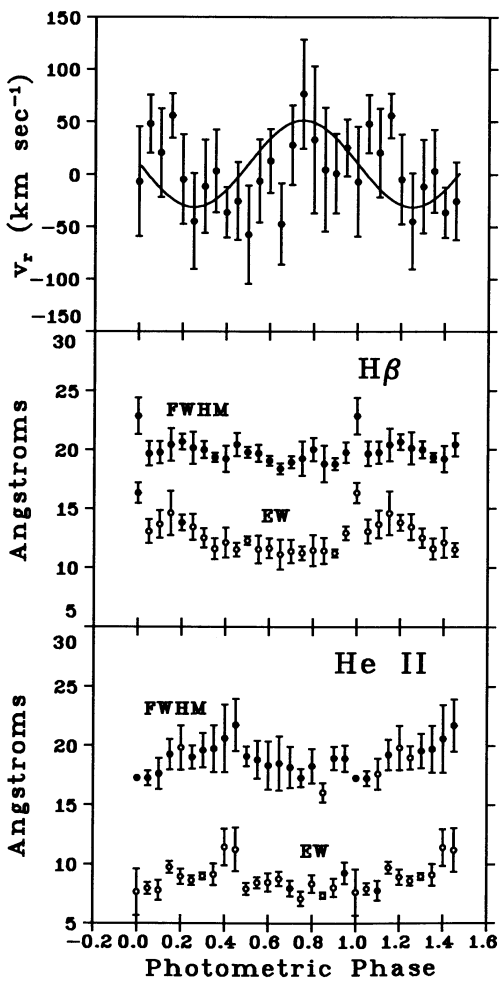

FIG. 6.—*Top panel:* "Fictitious" radial velocity curve generated by folding radial velocities on the photometric ephemeris of § 3.1. The solid line is the best-fit sinusoid with a semiamplitude of 41 km s^{-1}. *Middle panel:* FWHM (*filled ovals*) and equivalent width (EW; *open ovals*) for Hβ as a function of photometric phase. *Bottom panel:* FWHM (*filled ovals*) and equivalent width (*open ovals*) for He II λ4686 as a function of photometric phase.

the curve represents real contributions to the radial velocities we measure for CP Pup, the velocities themselves must be due to system dynamics distinctly separate from orbital motion. We corrected the velocities listed in Table 1 for this nonorbital contribution by first evaluating corrections based on each spectrum's photometric phase; second, applying these corrections to the individual spectra; and third, refolding the corrected spectra on the spectroscopic ephemeris. We found, however, that the contribution of the nonorbital motion to our estimates of K_1 for individual lines as well as combinations of lines is less than the uncertainty on our estimates.

3.3. *Emission-Line Profiles*

We used our spectroscopic ephemeris to co-add the 105 CP Pup spectra into 20 phase bins of width 0.05. Figure 7 shows the continuum-subtracted, average spectra for five spectroscopic phases. The spectra are dominated at all spectroscopic phases by the H Balmer lines, He I lines ($\lambda\lambda$4026, 4471), and He II lines ($\lambda\lambda$4541, 4686). Over an orbital period, all lines present seem to exhibit similar structural changes while maintaining full width at zero intensity velocity widths of 2000–4000 km s^{-1}. He II λ4686, as well as the C III/N III blend, are faintly double-peaked at $\phi_s = 0.0$, blueward peaked for $\phi_s = 0.2$, and redward peaked for $\phi_s = 0.6$. Similar behavior is also observed in the other lines as well. OWWG investigated whether the V/R variation they observed in the H Balmer and He II λ4686 lines is caused by a narrow "S"-wave. While they, like we, were unable to observe a narrow "S"-wave component, Dieters (1992) has observed such a narrow component in 1987 February data. The high-excitation lines visible in the spectrum of CP Pup are characteristic of old novae and magnetic CVs, and double-peaked emission lines in CVs are generally considered to be produced in an accretion disk (Smak 1969; Huang 1972; Smak 1981; Horne & Marsh 1986). The small velocity separation between the peaks in the double-peaked He II λ4686 line ($\approx$400–500 km s^{-1}) implies that while the high-excitation He lines are formed nearer the white dwarf than the H lines, they are formed at greater distances and with lower velocities than would be expected for a nonmagnetic CV in which the accretion disk reaches down to the white dwarf surface.

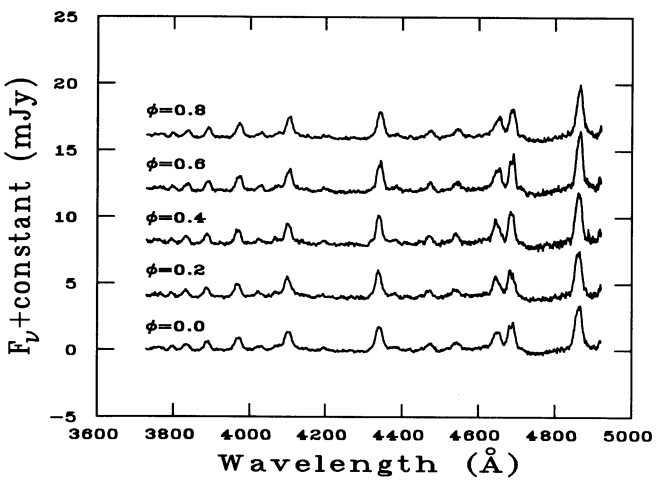

FIG. 7.—Continuum-subtracted, phase-binned spectra for five spectroscopic phases. The spectra were folded into 20 orbital phase bins using the spectroscopic ephemeris in § 3.2. Spectroscopic phase is shown above the corresponding spectrum. For presentation, a constant has been added in the ordinate to each spectrum except $\phi_s = 0.0$.

We calculated the FWHM and the equivalent width for Hβ and He II λ4686 using least-squares fits of Gaussians to the lines. The middle and bottom panels of Figure 5 show the behavior of the FWHM and the equivalent width for Hβ and He II λ4686 as a function of spectroscopic phase; the FWHM for each line displays periodic behavior, with maximum FWHM at approximately $\phi_s = 0.0$ and minimum FWHM at $\phi_s = 0.5$. Bianchini et al. (1985) observed modulation of the λ4686 line's equivalent width at the spectroscopic period, although the authors do not state the amplitude of the modulation they observed. We, however, see little or no modulation of equivalent width with spectroscopic phase for either Hβ or He II λ4686.

To investigate any possible modulation in the FWHM and equivalent widths for the Hβ and He II λ4686 lines at the photometric period, we also folded the spectra on our photometric ephemeris; we find statistically significant modulation in the FWHM and equivalent widths for both lines. In the middle and bottom panels of Figure 6 we plot FWHM and equivalent width as a function of photometric phase for Hβ and He II λ4686.

4. MASSES

We are unsure of CP Pup's orbital inclination except to note that no eclipses are observed. Duerbeck et al. (1987) assumed $i \leq 65°$ in their mass estimates but also estimated the angle of inclination $i = 30° \pm 5°$ using velocities of the system's nova ejecta. Their estimate is roughly the same as the $i = 35°$ of Szkody & Feinswog (1988), determined from the low amplitude of the ellipsoidal variations in system brightness due to heating of the secondary star. The lack of information concerning the secondary star necessitates the use of a mass-radius relation to estimate the secondary star's mass. While both theoretical and empirical M-R relations are used quite often to adopt the secondary star's mass, we are sobered by the potential errors involved in such estimates as discussed by Wade (1990).

We estimate the mass of the secondary star in the CP Pup system by assuming that the red dwarf fills its Roche lobe and that it obeys the M-R relation for the lower main sequence

$$\frac{R_2}{R_\odot} = \beta\left(\frac{M_2}{M_\odot}\right)^\alpha . \tag{2}$$

The value of the parameter β has been estimated to be in the range 0.87–1.00 for the lower main sequence (Faulkner 1971; Robinson 1976b). Theoretically, $\alpha \sim 1$ for the mass range $0.1 \lesssim M/M_\odot \lesssim 1.0$ (Faulkner 1971), while Patterson (1984) has empirically determined $\alpha = 0.88 \pm 0.02$ for the mass range $0.1 < M/M_\odot \lesssim 0.8$. We derive masses using both the theoretical and empirical values for α. By making the standard assumption that the spherical volume of the secondary star is equal to the volume of its Roche lobe, we can employ Paczyński's (1971) relation for small q, where $q = M_2/M_1$,

$$\frac{R_2}{a} = 0.46224\left(\frac{M_2}{M_1 + M_2}\right)^{1/3} . \tag{3}$$

Finally, we can use Kepler's third law and the two equations above to obtain for stars on the lower main sequence

$$\frac{M_2}{M_\odot} = \begin{cases} 3.37\beta^{-1.83}P^{1.22} & \text{empirical} \\ 2.71\beta^{-1.50}P^{1.00} & \text{theoretical} \end{cases} \tag{4}$$

where P is in days. Anticipating our mass estimates of CP Pup, we adopt $\beta = 0.87$. Using the theoretical M-R relation, we find $M_2 = 0.20\ M_\odot$, while use of the empirical M-R relation gives us $M_2 = 0.14\ M_\odot$. From Table 2, we see that most of the previously published values for M_2 are also $M_2 \approx 0.14\ M_\odot$. Adopting the empirical M_2, we use the mass function $f(M_2)$ to obtain an estimate of the mass of the white dwarf M_1. We find $f(M_2) = 0.020 \pm 0.0024\ M_\odot$, and for an orbital inclination $i \leq 65°$ we have $q \geq 0.77$ and $M_1 \leq 0.18\ M_\odot$. For $i = 35°$, we find $q = 6.4$ and $M_1 = 0.02\ M_\odot$!

As an alternate determination of the mass ratio q, we use the relationship between q and the ratio $(v_d \sin i)/K_1$, where $v_d \sin i$ is the projection of the gas velocity in the outer disk (Warner 1973; Shafter 1983). Adopting the recent calibration of Jurcevic & Honeycutt (1992), we associate $v_d \sin i$ with the FWHM of the Hβ line and find a mass-ratio range $0.5 \lesssim q \lesssim 0.9$, where the upper and lower limits are determined by the uncertainties on our estimates of K_1, the FWHM of the Hβ line, and the calibration. We note that this range includes our earlier lower limit $q \geq 0.77$ for an orbital inclination $i \leq 65°$; hence, we choose $q \sim 0.77$ as the mass ratio for our discussion of CP Pup.

Theoretical models of classical nova outbursts, which assume thermonuclear runaway in the accreted matter on the white dwarf as the outburst mechanism, have shown that the reduced degeneracy in white dwarfs of less than 0.5–0.6 $M_\odot$ makes it difficult to initiate outbursts on white dwarfs with masses in this range (Gallagher & Starrfield 1978; Livio & Truran 1987). Further, Smits's (1991) photoionization modeling of metal-enriched nova shells implies for CP Pup a white dwarf mass $M_1 \sim 1\ M_\odot$. We find that both our and other's empirical and theoretical estimates of the white dwarf mass for CP Pup are significantly below these theoretical limits.

As OWWG point out, there is really no portion of the mass determination process we have used that has not been criticized. And while we used an estimate of K_1 based on the H Balmer series for our mass estimates, we are aware of the great effect the large range in our K_1 estimates for individual lines (Table 1) can have on these mass estimates. However, OWWG's suggestion that the emission lines do not correctly represent the motion of the white dwarf is probably correct and echoes our earlier warning about the reliability of using emission-line radial velocity curves to estimate K_1.

5. DOPPLER TOMOGRAPHY

The spectrum of a CV contains information on the velocity field in the system; emission lines formed in accretion structures surrounding the white dwarf present profiles determined by the dynamical gas flow in the system. And the three-dimensional velocity field of the system is projected onto the observer's line of sight while the spectrum is captured. Thus, a series of spectra taken at different orbital phases provides one with projections of the system in velocity space from different vantage points. By combining these projections in a manner analogous to that employed in certain medical imaging systems, one can obtain an image of the system in velocity space, a so-called Doppler map or Doppler tomogram (Marsh & Horne 1988).

In the manner of Marsh et al. (1990) in their study of the dwarf nova U Geminorum, we constructed Doppler images of CP Pup by using the maximum-entropy inversion method described by Marsh & Horne (1988). In this method our data were fitted to a specified χ^2 based on the S/N ratio of our data. The fit was performed by maximizing the entropy in a uniform image until the image adequately represented the information contained in the spectroscopic data; we selected the proper image as did Marsh et al. (1990) by choosing the best trade-off between resolution and noise.

To construct the images, we cast the 105 continuum-subtracted spectra into 40 phase bins using our spectroscopic ephemeris. Figure 8 shows Doppler images of CP Pup in the light of Hβ and He II λ4686. The phase-binned, trailed spectra are shown in the top panels, and the corresponding Doppler images are shown below them. In our Doppler images, the X-axis is along the line of centers from the white dwarf to the secondary star, and the Y-axis is in the direction of the secondary star's orbital motion. The intensity of each pixel of the Doppler image, where black represents maximum intensity and white represents a small, positive intensity chosen to reduce the background in our gray-scale images, corresponds to the flux contribution from multiple "S"-waves of the form

$$V(\phi) = \gamma - V_X \cos(2\pi\phi) + V_Y \sin(2\pi\phi)\ . \quad (5)$$

We further minimized χ^2 by removing the γ-velocities from the appropriate spectra for the two nights separately; this reduced image blurring (Marsh & Horne 1988) and left us with a reduced $\chi^2 \approx 3$.

While the Doppler images of CP Pup do not show hot-spot emission, they do show disk emission. The disk emission is characterized in velocity space as a ring of emission roughly centered on the position of the white dwarf $(0, -K_1)$, while the hot spot would be located to the left of the secondary star's location $(0, K_2)$ on the velocity map (Horne 1991). High velocities in the Doppler images denote emission from near the white dwarf while low velocities correspond to regions further from the white dwarf. In the Hβ image of CP Pup, an extended emission "ringlet" is visible but in the wrong quadrant for a classical hot spot. A complete emission ring is also visible in the He II λ4686 image.

In an effort to understand the accretion structures in CP Pup that give rise to the emission visible in the Hβ image, we constructed Doppler maps using half-orbit data sets centered on eight orbital phases separated by $\phi_s = 0.125$. To improve our images' S/N and accentuate any fine structure that might be present, we combined the profiles of six of the H Balmer lines. Images constructed in this manner of a system for which all portions of the velocity field are visible at all times should be identical. But in their study of U Gem, Marsh et al. (1990) observed maximum hot spot intensity from orbital phase 0.75 to 0.00 and minimum at orbital phase 0.25, indicative of obscuration of the hot spot by the disk. The images of CP Pup in Figure 9 indicate the likely occultation or obscuration of emitting regions. The most intense emission regions in all Doppler images of Figures 8 and 9 appear to be concentrated on the side of the accretion disk opposite that of the secondary star with respect to the white dwarf.

6. DISCUSSION

6.1. *The Two Periods of CP Puppis*

Table 3 shows the various periods that have been determined for CP Pup. It seems apparent that two photometric period regions exist: one centered roughly at 0.068 day, the other at 0.062 day. Warner (1985a) was unable to eliminate either 0.06196 day or its 1 day alias 0.06614 day as probable periods, while Vogt et al. (1990) suggested that their observed range in period of 0.059 day to 0.070 day probably represented an oscillation of the photometric period about a mean of

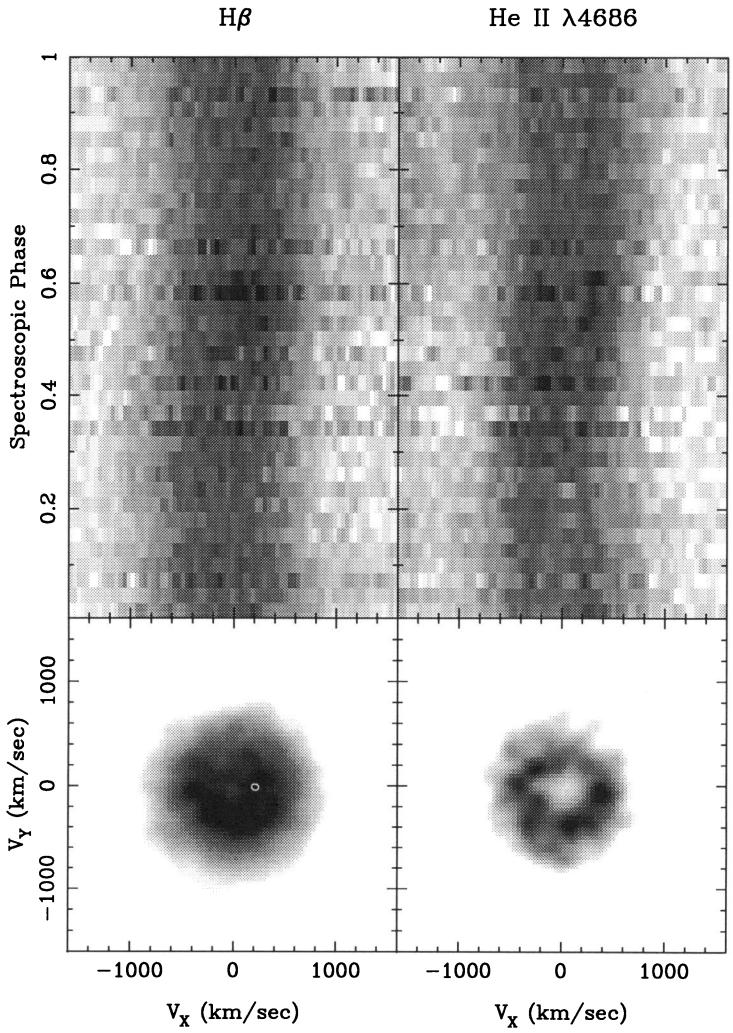

FIG. 8.—Observed spectra binned around given lines are displayed in the upper panels with spectroscopic phase along the ordinate and velocity relative to line centers along the abscissa. The Doppler images constructed from these data are shown in the panels below the trailed spectra.

≈0.063 day on a period of ≈3.8 days. Further, Szkody & Feinswog (1988), looking in the infrared for evidence of heating of the secondary star by the white dwarf in several CVs, found a best-fit double sinusoid with a period of 0.067 day for their CP Pup observations. The period analysis by OWWG, however, clearly indicated the existence of a photometric period of approximately 0.061–0.062 day, as did the *UBVRI* photometry of Diaz & Steiner (1991). Moreover, OWWG found that their spectroscopic period and photometric period were the same to within the errors. We note that OWWG's 0.061–0.062 day photometric period occurs at a minimum in our photometric power spectrum (Fig. 2*a*). All previously published photometric periods for CP Pup are near 0.062 day to within the errors while our result is clearly different. Though our photometry was performed using the continua of slit spectra with the emission lines excluded, not typical of normal photometry, we do not believe this should make the photometric period longer than the spectroscopic period. The reader, however, should keep this in mind. Finally, the light curve of CP Pup in Figure 1 and the modulation of line structure on two periods clearly demonstrate the existence of a photometric period distinctly different from the spectroscopic period for our data's epoch.

6.2. *Two Interpretations of the Data*

The existence of two periods for CP Pup and the modulation of radial velocities and line structure on those periods suggests that our data may be interpreted in light of either a DQ Her model or an SU UMa model. Modulation in line structure and strength on both the spectroscopic period and photometric period (Figs. 5 and 6) may be due to a line-emitting region in CP Pup that is being partially occulted periodically. Although we do not observe a narrow "S"-wave component in our spectra, the modulation of line width suggests that the lines may be combinations of at least two components: a narrow component and a broad component in a ratio that is a function of spectroscopic phase. In the trailed spectrograms of Figure 8, the double peaks of the He II λ4686 line appear more "filled in" for $\phi_s = 0.5$. That the lines are wide at $\phi_s = 0.0$ and narrow at $\phi_s = 0.5$ (Fig. 5) violates a fundamental premise of Doppler tomography which states that line profiles at opposite phases should be mirror images of one another. We interpret this modulation in line width as being due to the presence of a modulated, single-peaked component that is distinct from the persistent, double-peaked disk component. If the white dwarf were magnetic with a field strength sufficient to disrupt an accretion disk near the white dwarf and form accretion funnels

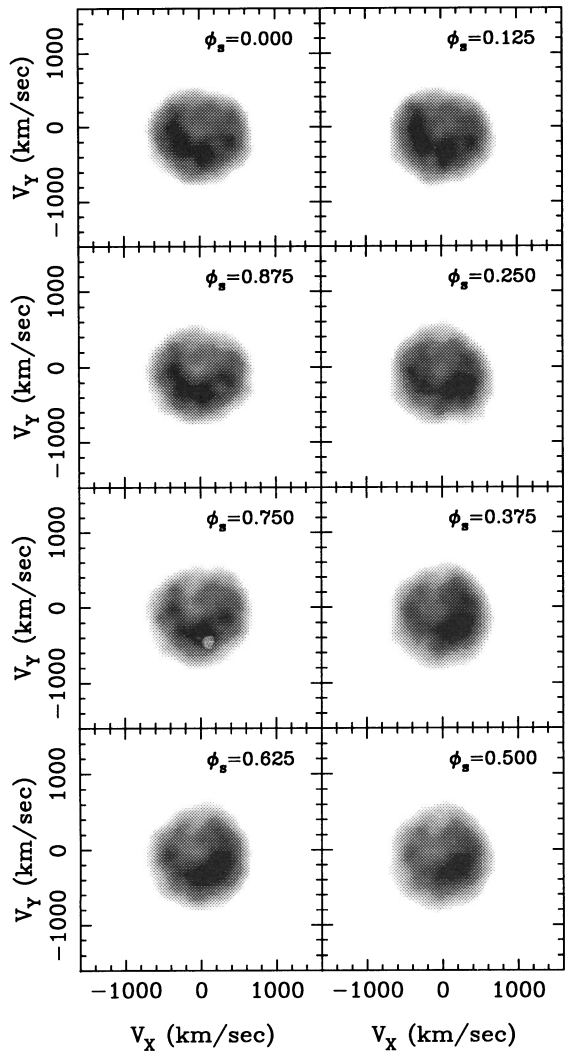

FIG. 9.—Doppler images of a combination of six H Balmer lines constructed using half-data sets centered on $\phi_s = 0.000$ to $\phi_s = 0.875$ and separated by 0.125.

($\sim 10^5$ G), one might observe periodic variations in line strength for different viewing aspects of the system. The occlusion of one of the funnels by the white dwarf itself would lead to line strengths and widths less than those when both funnels are visible. In SU UMa systems, however, the prograde precession of the tidally distorted accretion disk might lead to variations in line strengths and widths modulated on both the system's orbital period and the precession period of the distorted disk.

6.2.1. *The DQ Herculis Interpretation*

In a DQ Her CV, the magnetic field of the white dwarf is not sufficiently strong to produce a locked rotator. Like a lighthouse located on the edge of a merry-go-round, the radiation emitted from the magnetic poles on the white dwarf sweeps through space; we may view the accretion column(s) directly, or the column(s) may illuminate other moving structures in the system. Thus, photometric variations from a DQ Her system can occur on the white dwarf spin period, and/or on the orbtial period, and/or on the beat period.

A multiplicity in observed photometric periods is common for DQ Her objects (Warner 1985b). Periods corresponding to the white dwarf spin period P_{spin} and beat periods P_{beat} between P_{spin} and the orbital period, P_{orb}, may be visible in photometric observations (Warner 1985b; Wickramasinghe 1988). For all known DQ Her objects, $P_{spin} < P_{orb}$ (Berriman 1988), whereas for CP Pup, we apparently have $P_{spin} > P_{orb}$ if we assume that the observed photometric modulation is due to rotation of the white dwarf. The X-ray survey of Becker & Marshall (1981) showed that CP Pup, one of the brightest old novae, has a L_x of 9.5×10^{31} ergs s^{-1}, but they, like Eracleous, Patterson, & Halpern (1991) detected no significant modulation in the system's X-ray brightness. The observation of the 0.067 day infrared modulation (Szkody & Feinswog 1988), which might represent reprocessing of the X-ray radiation by structures in the system, supports our assertion that two photometric period regimes exist for CP Pup, but the lack of modulation in L_x suggests that the photometric variations may not be indicative of typical DQ Her–type behavior.

6.6.2. *The SU Ursae Majoris Interpretation*

If the system is in an SU UMa superoutburst state, another mechanism may lead to photometric variations. SU UMa systems are CVs characterized by short orbital periods, small-amplitude, semiperiodic outbursts, and larger amplitude, more periodic outbursts referred to as "superoutbursts" or "supermaxima" (Vogt 1980; Patterson et al. 1981). The superoutbursts generally last ~ 10 days and occur with a periodicity of a few hundred days to the extreme of 32.5 yr for WZ Sagittae (Patterson et al. 1981). During the superoutburst, modulation in an SU UMa system's brightness occurs with an amplitude of up to 0.5 mag and a periodicity 0.8%–9% longer than the orbital period (Molnar & Kobulnicky 1992). These modulations, called "superhumps," occur only during superoutbursts. Several theoretical models have been developed to explain the existence of superoutbursts, the concomitant superhumps, and the observed transition from normal outbursts to superoutbursts (Vogt 1982; Osaki 1985; Warner 1985c; Whitehurst 1988). The most viable model at the present time is that of Whitehurst (1988). In this model, the accretion disk develops an elliptical distortion that is approximately fixed in the binary's reference frame; orbital motion of the secondary star past the bulge of the elliptical disk leads to tidal heating in the outer disk and the observed superhump phenomenon. Slow prograde precession of the disk results in a superhump period P_{sh} slightly longer than the binary period.

Eighteen of the 19 SU UMa systems appear below the observed period gap for CVs (Molnar & Kobulnicky 1992). The periods measured for CP Pup also place it below the period gap. Further, a superhump period P_{sh}, longer than the spectroscopic period, is observed in the photometry of SU UMa systems. Models of SU UMa systems predict that a beat period P_{beat}, corresponding to the precession period P_{pre} of the tidally distorted accretion disk, should exist between P_{orb} and P_{sh}. In SU UMa systems, $q \lesssim 0.5$ (Molnar & Kobulnicky 1992), and during superoutbursts, $P_{sh} > P_{orb}$. Because superhumps are observed only during superoutbursts, CP Pup must have been in a state of superoutburst for decades to be interpreted as an SU UMa system, a feat not observed in known SU UMa systems. In their photometric study of the old nova V603 Aquilae, however, Patterson & Richman (1991) suggest that system's photometric modulation is similar to superhumps in SU UMa systems; as a possible explanation of their observations, the authors suggest that V603 Aql is in a state of enhanced mass transfer that produces "permanent super-

TABLE 3

SPECTROSCOPIC AND PHOTOMETRIC PERIODS FOR CP PUPPIS

Epoch	References	T[a]	Period (day)	Aliases (day)	Amplitude (mag)
1982 Dec	1	S	0.061425 ± 0.000025	...	...
1984 May	2	S	0.06115	...	...
1984 May	3	S	0.0605	0.0571	...
1985 Apr	4	S	0.06141 ± 0.00003	...	...
1986 Feb	5	S	0.0614215	...	...
1986 Feb	6	S	0.06142	...	...
1987 Jan	7	S	0.06129 ± 0.00001	...	...
1988 Mar	4	S	0.06148 ± 0.00005	...	...
1989 Mar	8[b]	S	0.0613750 ± 0.0000001	...	...
1985 Feb	9	P	0.06196	0.06614	±0.15
1985 Feb	4[c]	P	0.06198	...	...
1986 Jan	4	P	0.06138	...	...
1986 Feb	6	P	0.059 − 0.070 ± 0.002	...	...
1987 Jan	7	P	0.06834 ± 0.00007	0.07346, 0.06396	±0.15
1987 Dec	10[d]	P	0.067 ± 0.004	...	±0.25
1988 Mar	4	P	0.06154	...	< ±0.5
1990 Apr	11	P	0.0614	...	±0.042

[a] Type of observation: (S)pectroscopic or (P)hotometric.

[b] Data from 1982 December (Duerbeck et al. 1987), 1984 May (Bianchini et al. 1985), 1988 March, and 1989 March combined for analysis.

[c] Reanalyzed Warner 1985a data.

[d] Infrared observations.

REFERENCES.—(1) Duerbeck et al. 1987; (2) Bianchini et al. 1985; (3) Friedjung et al. 1988; (4) O'Donoghue et al. 1989; (5) Barrera & Vogt 1989; (6) Vogt et al. 1990; (7) this study; (8) Bianchini et al. 1990; (9) Warner 1985a; (10) Szkody & Feinswog 1988; (11) Diaz & Steiner 1991.

humps." The so-called standstill of Bianchini (1990) describes the fact that since the nova outburst, CP Pup has been about 2 mag brighter than during its prenova state. This may support the assertion of enhanced mass transfer and/or superoutburst behavior in CP Pup. Also, in our data CP Pup's blue light is modulated with a semiamplitude of approximately 0.15 mag, consistent with superoutburst amplitudes. Szkody & Feinswog (1988) in the infrared and Diaz & Steiner (1991) in the *B* band observed brightness variations of 0.025 mag and 0.042 mag, respectively, while Warner (1985a) in white light, like we in the *B* band, observed variations of 0.15 mag. In addition, OWWG observed variations up to 40% of mean system brightness during one of their runs.

Our estimates on the masses and mass ratio in CP Pup, though admittedly uncertain for the reasons discussed in § 4, may place CP Pup in the parameter domain of SU UMa systems. Molnar & Kobulnicky (1992) show that period excess, $\Delta P/P_{\rm orb} = (P_{\rm sh} - P_{\rm orb})/P_{\rm orb}$, in SU UMa systems is significantly correlated with the mass ratio and the authors go on to show that the correlation is consistent with a strictly monotonic relationship as predicted by Whitehurst & King (1991). If we use our estimates of $q \geq 0.77$ and $\Delta P/P_{\rm orb} = 0.11$ to place CP Pup on Molnar & Kobulnicky's (1992) Figure 2, we find that the strict monotonic relationship is preserved. Unfortunately, $q \geq 0.77$ is much greater than the upper limit $q \leq 0.22$ given by the Whitehurst (1988) model for the development of SU UMa–type behavior, although seven of the SU UMa systems included in Molnar & Kobulnicky's (1992) work have mass ratios greater than this upper limit. The authors state that all SU UMa systems with reliable mass ratio estimates have mass ratios less than the Whitehurst limit; nevertheless, the existence of so many exceptions to this limit mildly supports the suggestion that CP Pup may also be of the SU UMa subclass of CVs.

A final bit of evidence that may also strengthen the SU UMa interpretation is the existence of other CVs, known to be SU UMa stars, with accretion disk enhancement similar to that which we observe in the Doppler tomograms of Figures 8 and 9. In their study of the dwarf nova WZ Sge, Gilliland, Kemper, & Suntzeff (1986) observed maximum *V*/*R* ratios at about orbital phase 0.3 rather than ≈0.7 as predicted by the standard hot spot model in which the mass transfer stream impacts the outer edge of the accretion disk. This observation implies the existence of an emission region on the side of the accretion disk

TABLE 4

EVIDENCE FOR AND AGAINST DQ HERCULIS AND SU URSAE MAJORIS CLASSIFICATION OF CP PUPPIS

DQ HERCULIS SUBCLASS		SU URSAE MAJORIS SUBCLASS	
For	Against	For	Against
Two periods High-excitation lines Modulation of EW and FWHM on P_p, P_s	$P_p > P_s$[a]	Two periods $P_p > P_s$ $P_s < 2$ hr Small mass ratio $\Delta m \lesssim 0.5$ mag Emission from backside of disk	P_p 11% longer than P_s is extreme Protracted superoutburst is extreme

[a] P_p is the photometric period, and P_s is the spectroscopic period.

opposite the hot spot. Similarly, Shafter, Szkody, & Thorstensen (1986) observed enhancement of the backside of the accretion disk in the dwarf nova SW Ursae Majoris. While SW UMa is suspected to be a DQ Her star (Shafter et al. 1986), it is known to also be an SU UMa star like WZ Sge (Molnar & Kobulnicky 1992).

6.2.3. *Summary of Evidence for Both Interpretations*

Both the SU UMa phenomenon and the DQ Her phenomenon have characteristics that resemble the two-period behavior of CP Pup. It is central to understanding the nature of CP Pup that this ambiguity be addressed. Therefore, we summarize the evidence for each interpretation in Table 4. We must also point out that if CP Pup is eventually shown conclusively to be a member of either subclass, this system will be one of the most unusual members of that subclass.

7. CONCLUSIONS

Our analysis of spectrophotometric data of the old nova CP Pup suggest that the system may be interpreted as either a DQ Her system or an SU UMa system. We have determined for the first time two distinct, yet simultaneous, periods for the system. While we associate the spectroscopic period with CP Pup's orbital period, we cannot firmly identify the photometric period with the white dwarf spin period as is often the case for DQ Her systems or with the superhump period for SU UMa systems during superoutburst. Our mass estimates for the white dwarf in CP Pup, like those of other authors, are, according to models, too low to support a nova outburst.

The observed modulations of up to 0.5 mag in CP Pup's brightness, a spectroscopic period that places the system below the period gap, and a photometric period longer than the spectroscopic period are evidence of SU UMa–type behavior. Further, in Doppler tomographic images we constructed by folding the spectra on the spectroscopic period, we observe a ringlet of emission that corresponds to enhanced disk emission from the side of the accretion disk opposite the secondary star with respect to the white dwarf. Similar enhancement of the rear of the accretion disk has been observed in at least two dwarf novae systems; this suggests a possible connection between CP Pup and dwarf novae, the class of CVs associated with SU UMa–type behavior. The existence of two periods for the system, however, along with the presence of high-excitation lines and modulation of line structure on the spectroscopic and photometric periods also supports the assertion that CP Pup is a DQ Her–type CV.

We would like to acknowledge the advice and assistance of Tom Marsh in the construction of Doppler tomograms and the helpful comments of Stefan Dieters and Dick Durisen in the writing of this paper. We thank the staff of CTIO for their help in obtaining the observations of CP Pup. This research has made use of the Simbad data base, operated at CDS, Strasbourg, France. K. H. is grateful to NASA for research funding under grant NAGW-2678. J. C. W. and R. K. H. acknowledge the support of the National Science Foundation in this research.

REFERENCES

Barrera, L. H., & Vogt, N. 1989, Rev. Mexicana Astron. Af., 19, 99
Bath, G. T., & Pringle, J. E. 1985, in Interacting Binary Stars, ed. J. E. Pringle & R. A. Wade (Cambridge: Cambridge Univ. Press), 177
Becker, R. H., & Marshall, F. E. 1981, ApJ, 244, L93
Berriman, G. 1988, in Polarized Radiation of Circumstellar Origin, ed. G. V. Coyne, S. J., A. F. J. Moffat, S. Tapia, A. M. Magalhães, R. E. Schulte-Ladbeck, & D. T. Wickramasinghe (Vatican City State: Vatican Observatory), 281
Bianchini, A. 1990, in Physics of Classical Novae, ed. A. Cassatella & R. Viotti (Berlin: Springer-Verlag), 13
Bianchini, A., Friedjung, M., & Sabbadin, F. 1985, Inf. Bull. Var. Stars, No. 2650
———. 1990, in Physics of Classical Novae, ed. A. Cassatella & R. Viotti (Berlin: Springer-Verlag), 61
Cropper, M. 1986, MNRAS, 222, 225
Diaz, M. P., & Steiner, J. E. 1991, PASP, 103, 964
Dieters, S. 1992, private communication
Duerbeck, H. W., Seitter, W. C., & Duemmler, R. 1987, MNRAS, 229, 653
Eracleous, M., Patterson, J., & Halpern, J. 1991, ApJ, 370, 330
Faulkner, J. 1971, ApJ, 170, L99
Friedjung, M., Bianchini, A., & Sabbadin, F. 1988, Messenger, No. 52, 49
Gallagher, J. S., & Starrfield, S. 1978, ARA&A, 16, 171
Gilliland, R. L., Kemper, E., & Suntzeff, N. 1986, ApJ, 301, 252
Haefner, R. 1981, Inf. Bull. Var. Stars, No. 2045
Horne, K. 1991, in Fundamental Properties of Cataclysmic Variable Stars, ed. A. W. Shafter (San Diego: San Diego State University Publication), in press
Horne, K., & Marsh T. R. 1986, MNRAS, 218, 761
Huang, S. 1972, ApJ, 171, 549
Jurcevic, J., & Honeycutt, R. K. 1992, private communication
Kaitchuck, R. H., Hantzios, P. A., Kakaletris, P., Honeycutt, R. K., & Schlegel, E. M. 1987, ApJ, 317, 765
Liebert, J., & Stockman, H. S. 1985, in Cataclysmic Variables and Low-Mass X-Ray Binaries, ed. D. Q. Lamb & J. Patterson (Dordrecht: Reidel), 151
Livio, M., & Truran, J. W. 1987, ApJ, 318, 316
Marsh, T. R., & Horne, K. 1988, MNRAS, 235, 269
Marsh, T. R., Horne, K., Schlegel, E. M., Honeycutt, R. K., & Kaitchuck, R. H. 1990, ApJ, 364, 637
Molnar, L. A., & Kobulnicky, H. A. 1992, ApJ, 392, 678
O'Donoghue, D., Warner, B., Wargau, W., & Grauer, A. D. 1989, MNRAS, 240, 41 (OWWG)
Osaki, Y. 1985, A&A, 144, 369
Paczyński, B. 1971, ARA&A, 9, 183
Patterson, J. 1984, ApJS, 54, 443
Patterson, J., McGraw, J. T., Coleman, L., & Africano, J. L. 1981, ApJ, 248, 1067
Patterson, J., & Richman, H. 1991, PASP, 103, 735
Payne-Gaposchkin, C. 1957, The Galactic Novae (Amsterdam: North-Holland)
Robinson, E. L. 1976a, ARA&A, 14, 119
———. 1976b, ApJ, 203, 485
Schmidt, G. D., & Liebert, J. 1987, Ap&SS, 131, 549
Schmidt, G. D., & Stockman, H. S. 1991, ApJ, 371, 749
Schneider, D. P., & Young, P. 1980, ApJ, 238, 946
Shafter, A. W. 1983, Ph.D. thesis, Univ. of California, Los Angeles
Shafter, A. W., Robinson, E. L., Crampton, D., Warner, B., & Prestage, R. M. 1990, ApJ, 354, 708
Shafter, A. W., & Szkody, P. 1984, ApJ, 276, 305
Shafter, A. W., Szkody, P., & Thorstensen, J. R. 1986, ApJ, 308, 765
Smak, J. 1969, Acta Astr., 19, 155
———. 1981, Acta Astr., 31, 395
Smits, D. P. 1991, MNRAS, 248, 217
Stockman, H. S., Schmidt, G. D., & Lamb, D. Q. 1988, ApJ, 332, 282
Szkody, P., & Feinswog, L. 1988, ApJ, 334, 422
Vogt, N., Barrera, L. H., Barwig, H., & Mantel, K.-H. 1990, in Accretion-Powered Compact Binaries, ed. C. W. Mauche (Cambridge: Cambridge Univ. Press), 391
Vogt, N. 1980, A&A, 88, 66
———. 1982, ApJ, 252, 653
Wade, R. A. 1990, in Accretion-Powered Compact Binaries, ed. C. W. Mauche (Cambridge: Cambridge Univ. Press), 181
Wade, R. A., & Ward, M. J. 1985, in Interacting Stars, ed. J. E. Pringle & R. A. Wade (Cambridge: Cambridge Univ: Press), 129
Warner, B. 1973, MNRAS, 162, 189
———. 1983, in IAU Colloq. 72, Cataclysmic Variables and Related Objects, ed. M. Livio & G. Shaviv (Dordrecht: Reidel), 155
———. 1985a, MNRAS, 217, 1P
———. 1985b, in Cataclysmic Variables and Low-Mass X-Ray Binaries, ed. D. Q. Lamb & J. Patterson (Dordrecht: Reidel), 269
———. 1985c, in Interacting Binaries, ed. P. P. Eggleton & J. E. Pringle (Dordrecht: Reidel), 367
Weaver, H. F. 1944, ApJ, 99, 280
Whitehurst, R. 1988, MNRAS, 232, 35
Whitehurst, R., & King, A. 1991, MNRAS, 249, 25
Wickramasinghe, D. T. 1988, in Polarized Radiation of Circumstellar Origin, ed. G. V. Coyne, S. J., A. F. J. Moffat, S. Tapia, A. M. Magalhães, R. E. Schulte-Ladbeck, & D. T. Wickramasinghe (Vatican City State: Vatican Observatory), 3